# FISSION OF $^{182,183}$Hg NUCLEI AT ENERGIES AROUND THE COLOUMB BARRIER*

M. Cheralu[a], Y.S. Mukhamejanov[a,b,c], E.M. Kozulin[a]
G.N. Knyazheva[a], I.M. Itkis[a], T. Banerjee[a], I.N. Diatlov[a]
D. Kumar[a], N.I. Kozulina[a], K.V. Novikov[a], A.N. Pan[a,b]
I.V. Pchelintsev[a], R.S. Tikhomirov[a], I.V. Vorobiev[a], M. Maiti[d]
R. Prajapat[d], R. Kumar[d], G. Sarkar[d], W.H. Trzaska[e]
P.P. Singh[f], R.N. Sahoo[f], E. Vardaci[g], A. Andreev[h]
A. Mitu[i], I. Harca[i]

[a]Joint Institute for Nuclear Research, Dubna, Russia
[b]Institute of Nuclear Physics, Almaty, Kazakhstan
[c]al-Farabi Kazakh National University, Almaty, Kazakhstan
[d]Department of Physics, Indian Institute of Technology Roorkee, Roorkee, India
[e]Department of Physics, University of Jyväskylä, Finland
[f]Department of Physics, Indian Institute of Technology Ropar, Punjab, India
[g]Dipartimento di Scienze Fisiche and INFN, Napoli, Italy
[h]Department of Physics, University of York, York YO10 5DD, UK
[i]IFIN-HH, Bucharest-Măgurele, Romania

*(Received November 19, 2021; accepted November 22, 2021)*

Asymmetric fission of mercury nuclei was initially observed in the low-energy region. In recent years, several experiments have been performed in this direction to investigate the asymmetric behaviour of Hg nuclei which supported the influence of shell effects on the asymmetric fission process. An experiment was performed using the CORSET setup. We investigated mass and energy distributions of fragments and fission characteristics of prolately-deformed $^{182}$Hg and oblately-deformed $^{183}$Hg nuclei formed in the $^{40}$Ca+$^{142,143}$Nd reactions at three different beam energies — $E_{\rm lab}$ = 172, 192, and 212 MeV. We found no huge variation in mass–energy distributions of $^{182}$Hg and $^{183}$Hg at any of the measured energies. This gives us an outlook regarding the influence of shell structure, charge radii deformation, and factors associated with the potential energy surface that is responsible for fission in the Hg region.

DOI:10.5506/APhysPolBSupp.14.741

* Presented at III International Scientific Forum "Nuclear Science and Technologies", Almaty, Kazakhstan, September 20–24, 2021.

## 1. Introduction

Nuclear fission has been widely studied for several years. It is a unique tool that helps in exploring the nuclear potential energy landscape and several properties of the nucleus. Earlier fission was observed only in symmetric mode and analysed on the basis of the Liquid Drop Model (LDM). Numerous experimental studies have shown that at low excitation energies, actinides with masses of up to $A \approx 256$ undergo mainly asymmetric fission [1]. This analytically showed that fission could be both symmetric and asymmetric. The asymmetric behaviour was due to shell effects, which vanish with an increase in excitation energy. It was observed that fission attains a complicated picture at low excitation energy where shell effects play a prominent role [2].

Contrary to actinides, nuclei in the Pb region mainly undergo symmetric fission at low excitation energies. Nevertheless, the study [2, 3] done earlier had shown flat-top or even double-humped mass distributions for several nuclei ($^{195}$Au, $^{198}$Hg, and $^{201}$Tl). Recently, an experimental study of $^{180}$Hg has shown asymmetric fission-fragment mass distribution [4], which led to an intensive study of the fission properties of nuclei in this region, where the major concern was to investigate if similar behaviour is observed in the neighbourhood of $^{180}$Hg. The $^{180}$Hg nucleus showed a clearly pronounced mass-asymmetric fission with most probable fragment masses around 80 and 100 amu, although it was natural to expect two semi-magical $^{90}$Zr ($Z = 40$, $N = 50$) fragments. In recent years, several experiments [5–9] have been performed in this direction to investigate the asymmetric behaviour of Hg nuclei which supported the influence of shell effects on the asymmetric fission process. Theoretical studies [10, 11] performed on the basis of the five-dimensional potential-energy surface using the macroscopic–microscopic model have been able to explain this typical behaviour exhibited by $^{180}$Hg. Möller [10] had applied the "random walk" method on the five-dimensional potential-energy surface for 982 nuclei and came out with a detailed theoretical study that showed asymmetric fission-fragment mass distributions in the actinide and sub-lead regions.

In our current study, we have analysed the fission of prolately-deformed $^{182}$Hg and oblately-deformed $^{183}$Hg at three different energies around the Coulomb barrier (172, 192, and 212 MeV). Prolate deformation is a familiar mode in the nuclear chart because collective behaviour of particles appears away from the closed shell, as nucleon–nucleon correlation increases the minimum energy configuration of nucleus leading to small deformation [12], but oblate deformation is a local observation made only in $^{182,183,185}$Hg nuclei. Prolately deformed are the nuclei that have their symmetric and rotational axis parallel to each other, and oblately-deformed nuclei have their symmetric and rotational axis perpendicular to each other [13]. Different de-

formation results in varying shell structure and nucleon distribution which are responsible for the fission barrier height, within the nucleus affecting the behaviour of fission fragment mass distribution. A recent study [12] in this region has shown that $^{183}$Hg has a larger charge radius in comparison with $^{182}$Hg. Hence, the current study aimed at investigating the behaviour of the fission-fragment mass and energy distributions of two differently deformed nuclei.

## 2. Experimental setup

The experiment was conducted at the Flerov Laboratory of Nuclear Reactions using $^{40}$Ca beam extracted from U-400 cyclotron at 172, 192, and 212 MeV with an energy resolution of 2%. Beam intensities on targets were 80–100 nA. The layers of $^{142,143}$Nd with a thickness of 225 $\mu$g cm$^{-2}$ and 196 $\mu$g cm$^{-2}$, respectively, deposited on carbon backings of 30 $\mu$g cm$^{-2}$ were used as targets. During the experiment, the target backings faced the beam. The binary reaction products were measured using the double-arm time-of-flight CORSET spectrometer [14]. Each arm of the spectrometer consisted of a compact start detector and position-sensitive stop detector based on microchannel plates. The arms of the spectrometer were arranged symmetrically with respect to the beam axis at an angle of 60°. The angle of the capture of each arm was ±19° in the reaction plane, ±8° off the reaction plane. The target was placed at an angle of 90° with respect to the beam axis. The angular resolution of the spectrometer was 0.3°, and the time resolution was 150 ps. The mass and energy resolutions of the spectrometer under these conditions were ±1.5 amu and ±3 MeV, respectively. Primary masses, velocities, energies, and angles of reaction products in the center-of-mass system were calculated from the measured velocities and angles using the momentum and mass conservation laws.

## 3. Results and discussion

The mass total kinetic energy (M-TKE) distributions of primary binary fragments obtained in the $^{40}$Ca +$^{142,143}$ Nd reactions at three beam energies are shown in Fig. 1. Considering the threshold requisite for quasi-fission to be Z1Z2 ∼ 1400, the maximum obtained for the reactions under investigation is Z1Z2 ∼ 1200. This makes CN formation favourable yield. Experiments were conducted near the Coulomb barrier in order to obtain CNs at least available excitation energy. In the pre-actinide region, pre-scission neutron and proton calculated using the Hilscher systematics [15] and NRV code [16], respectively, are low and may be neglected in the current study.

Unlike the actinide region, the influence of the descent from the fission barrier to the scission point in the pre-actinide region is least. In this region, fission properties of the nuclei are majorly determined at its saddle

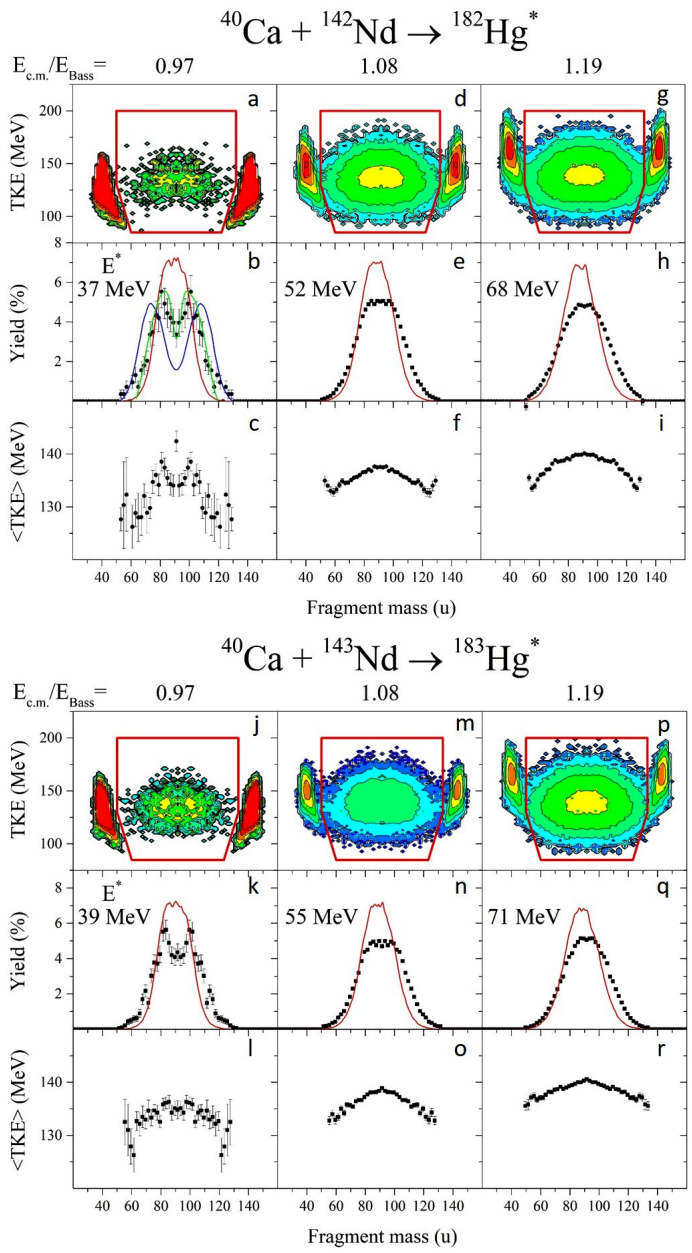


Fig. 1. The mass total kinetic energy (M-TKE) distributions of primary binary fragments obtained in the $^{40}$Ca +$^{142,143}$ Nd reactions. Mass yields and theoretical calculations: Möller calculation (solid blue/black line) [19], Andreev (solid green/light grey line) [20], GEF calculations (solid red/grey line) [21].

point and are influenced by the excitation energy [6]. Since two fragments are produced per fission, we have normalized mass yield to 200%. In the M-TKE distributions, the reaction products with masses close to those of the projectile and target are associated with elastic and quasi-elastic events and were not considered in the present analysis. The mass yields are shown in Figs. 1 and 2. It is clearly seen that at similar excitation energies, the mass and energy distributions of fission fragments look very much alike for the both reactions. At low excitation energies, the mass distributions have a flat-top shape and are far from being a single Gaussian. At higher excitation energies, the mass distributions become more symmetric. It is well known that the kinetic energy of fission fragments is mainly determined by the Coulomb repulsion of fragments formed at the scission point. Following the LDM, the average kinetic energy has a parabolic dependence on fragment mass and barely changes with excitation energy and angular momentum. Analysis of the obtained experimental data was done under the assumption that both symmetric and asymmetric fission modes contribute to mass and TKE distributions. We assume that the fission-fragment mass distributions of the pre-actinide nuclei can be described as a sum of symmetric (S) and several asymmetric modes (A1, A2, A3) [18], each asymmetric mode being a sum of two Gaussians centred at fragment masses 82.5(±1) and 100(±1), 76(±1) and 106(±1), 66(±1) and 116(±1) amu, respectively. Since the kinetic energy of fragments originates mainly from the Coulomb repulsion at the scission point, the TKE value depends on the distance $d$ between the centres of the formed fragments. It allows to estimate the shape at scission for various modes: the A2 mode is more compact than the LDM one, while for the A1 mode the shape is more elongated.

This asymmetric component centred at 66(±1), 116(±1), 76(±1), and 106(±1) amu is expected due to the influence of closed proton shells. The yield of the component slightly decreases with increasing excitation energy and is considerably lower compared to the asymmetric component centred at 81(±1) and 101(±1) amu, whose yield is observed to be sharply diminishing with an increase in excitation energy. This asymmetric mode can be caused by the influence of a deformed proton shell at $Z = 45$. For the lowest energy of 172 MeV (about 7 MeV lower than the Coulomb barrier) corresponding to the excitation energy $E^* = 37$ MeV for $^{182}$Hg and 39 MeV for $^{183}$Hg, the mass distributions in Fig. 2 involve major contribution of the A3 asymmetric component. The contribution of the symmetric component at this energy is very low. As it is seen from Fig. 2, at the beam energy of 192 MeV ($E^* = 52$ MeV and 55 MeV for $^{182,183}$Hg, respectively), the contribution of the asymmetric components decreased significantly, whereas the contribution of the symmetric one is about 70%. At the energy of 212 MeV, which is 24 MeV above the Coulomb barrier ($E^* = 68$ MeV and 71 MeV for $^{182,183}$Hg, respectively), symmetric fission is the main process, although some

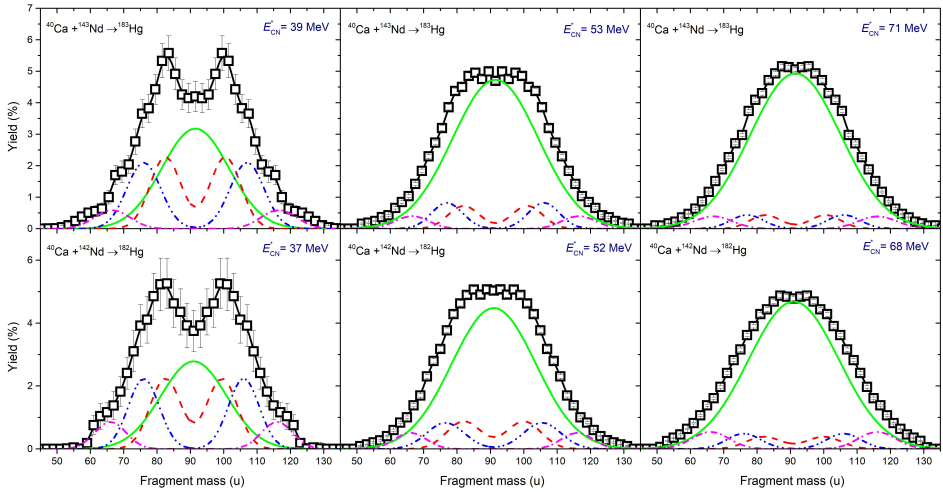


Fig. 2. The mass yields obtained in the $^{40}$Ca+$^{142,143}$Nd reactions. The lines correspond to the decompositions of mass yields into symmetric (green/solid lines), asymmetric A1 (red/dashed line), asymmetric A2 (blue/dash-dot-doted line), and asymmetric A3 (pink/dash-doted line) modes.

yield of asymmetric fission is still observed. In Fig. 1 (b), the experimental mass distributions are also compared with the theoretical calculations by Möller [19] at the excitation energies of 40 MeV. Möller has made a theoretical study of fission of even mercury nuclei where he has included Brownian Metropolis shape motion for the nuclei propagating from the saddle to the scission point in the potential energy surface (PES) which showed remarkable asymmetric fission behaviour. The microscopic effect responsible for asymmetric fission is observed experimentally and theoretically. The shift of asymmetric peaks in the theoretical calculation with respect to the experimental observation is said to be due to the confined fission valley in the sub-lead region that raises difficulty in calculating potential energy surface parameters. The ridges present in the PES could be accountable for the fission of Hg nuclei when the motion of nuclei as a "random walk" is considered. Later in 2013, with an improved scission-point point model, the mass distributions for even Hg isotopes with mass numbers $A = 174$ to 196 are calculated [20]. In Fig. 1 (b), the mass distribution obtained at the excitation energy of 20 MeV is compared with our data at the excitation energy of 37 MeV, and we obtain good agreement with the recent calculation. As it is seen in Fig. 2, the measured mass distributions are well reproduced by the consideration of symmetric and asymmetric modes at all three studied energies. It is found that the symmetric mode is growing with increasing excitation energy, hence the asymmetric modes are washing out with the raise of excitation energy in the sub-lead region of nuclei.

As we can see in Fig. 3, the observed values of TKE are about 7 MeV lower than the value estimated using the Viola systematics [17]. In spite of the difference in shape deformations of $^{182}$Hg and $^{183}$Hg at their ground states, the fission fragment mass and TKE distributions are nearly identical. Thus, it can be concluded that the shape-staggering effect in $^{182,183}$Hg does not affect significantly the fission mass and TKE distributions at energies considered.

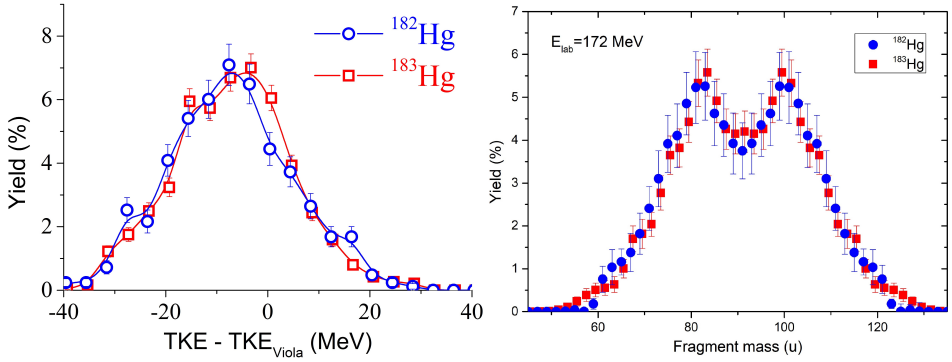


Fig. 3. The TKE distributions, mass yields of $^{182,183}$Hg fission fragments.

## 4. Conclusions

The mass and energy distributions were measured within the 37–96 MeV excitation energy range for $^{182,183}$Hg, populated using the reactions $^{40}$Ca+ $^{142,143}$Nd, respectively. We obtained identical results for both $^{182}$Hg and $^{183}$Hg nuclei which have different deformation structure at the ground state and varying charge radii with respect to one another. To analyse the experimental mass distributions, we have considered symmetric and three asymmetric modes. It was found that as the beam energy increases, the contribution of the asymmetric components decreases and mass distribution tends to attain a symmetric shape. Analysis of the experimental data showed that the asymmetric modes are present in the fission of $^{182,183}$Hg up to the excitation energy of about 70 MeV. Similarly, to the fission of actinides, the contribution of a symmetric component in mass distribution increases with increasing the excitation energy. However, the mechanism of asymmetric fission of Hg is different from the actinide region. Contrary to the fission of actinides, in the sub-lead region, asymmetric fission tends to have lower energy than symmetric fission. For asymmetric fission, the most probable heavy- and light-fragment masses were found to be 101 and 81 amu for $^{182}$Hg, and 102 and 81 amu for $^{183}$Hg. This may be caused by the influence of a deformed proton shell at $Z = 45$. The asymmetric component with the peaks at mass 114 amu and complementary one caused by the closed proton

shells $Z = 50$ and $Z = 28$ was also found for the both fissioning nuclei. Our study showed similar behaviour of prolately-deformed $^{182}$Hg and oblately-deformed $^{183}$Hg nuclei, the differences in the mass yield of both the reactions are shown in Fig. 3. The influence of deformation on the fission-fragment mass distribution at higher energies needs further investigation.

## REFERENCES


[1] F. Goennenwein, «Mass, Charge, and Kinetic Energy of Fission Fragments», in: «The Nuclear Fission Process», *CRC Press, Inc.*, Boca Raton, FL 1991, p. 287.

[2] M.G. Itkis *et al.*, *Yad. Fiz.* **52**, 944 (1990).

[3] M.G. Itkis *et al.*, *Yad. Fiz.* **53**, 1225 (1991).

[4] A.N. Andreyev *et al.*, *Phys. Rev. Lett.* **105**, 252502 (2010).

[5] D. Kumar *et al.*, *Bull. Russ. Acad. Sci.: Phys.* **84**, 1001 (2020).

[6] K. Nishio *et al.*, *Phys. Lett. B* **748**, 89 (2015).

[7] E. Prasad *et al.*, *Phys. Rev. C* **91**, 064605 (2015).

[8] R. Tripathi *et al.*, *Phys. Rev. C* **92**, 024610 (2015).

[9] I. Tsekhanovich *et al.*, *Phys. Lett. B* **790**, 583 (2019).

[10] P. Möller, J. Randrup, *Phys. Rev. C* **91**, 044316 (2015).

[11] A.V. Andreev, G.G. Adamian, N.V. Antonenko, *Phys. Rev. C* **93**, 034620 (2016).

[12] B.A. Marsh *et al.*, *Nature Phys.* **14**, 1163 (2018).

[13] D.J. Rowe, «Nuclear Collective Motion. Models and Theory», 1970.

[14] E.M. Kozulin *et al.*, *Instrum. Exp. Tech.* **51**, 44 (2008).

[15] D. Hilscher, H. Rossner, *Ann. Phys. Fr.* **17**, 471 (1992).

[16] A.V. Karpov *et al.*, *Nucl. Instrum. Methods Phys. Res. A* **859**, 112 (2017); `http://nrv.jinr.ru/nrv`

[17] V.E. Viola, K. Kwiatkowski, M. Walker, *Phys. Rev. C* **31**, 1550 (1985).

[18] A.A. Bogachev *et al.*, *Phys. Rev. C* **104**, 024623 (2021).

[19] P. Möller *et al.*, *Phys. Rev. C* **85**, 024306 (2012).

[20] A.V. Andreev, G.G. Adamian, N.V. Antonenko, A.N. Andreyev, *Phys. Rev. C* **88**, 047604 (2013).

[21] General description of fission observables: GEF model code, K.-H. Schmidt, B. Jurado, C. Amouroux, C. Schmitt, *Nucl. Data Sheets* **131**, 107 (2016).